

Large eddy simulation of dispersion in free surface shear flow

Simulation des grandes échelles de dispersion dans les écoulements cisailés à surface libre

C.W. LI & J.H. WANG, *Department of Civil & Structural Engineering, The Hong Kong Polytechnic University, Hong Kong*

ABSTRACT

Wastewater and waste heat are frequently discharged into ambient water and affect the water quality there. An accurate evaluation of the turbulent mixing and dispersion processes is one of the key factors for assessing the environmental impact of these discharges. To achieve this objective a three-dimensional numerical model incorporating the method of Large Eddy Simulation has been developed. In this method the large scale turbulence is computed explicitly and the subgrid scale turbulence is modelled. The empiricism incurred for the specification of the dispersion and turbulent mixing coefficients is thus reduced to minimal. The governing equations are split into three parts in the finite difference solution: advection, dispersion and propagation. The advection part is solved by a characteristics-based scheme. The dispersion part is solved by the central difference method and the propagation part is solved implicitly by using the Gauss-Seidel iteration method. The model has been applied to simulate a continuous line source in free surface shear flow. The computed results demonstrate the existence of the non-Fickian diffusion and dispersion region close to the source. Further downstream the transverse diffusion process obeys Fick's Law and the transverse diffusion coefficient is in agreement with the empirical value measured in laboratory. The initial non-Fickian diffusion and dispersion region is further analysed based on the coherence of the velocity data. The dispersion coefficient is found to follow the Okubo's $4/3$ power law, but with a much larger coefficient owing to the shear effect.

RÉSUMÉ

Les eaux usées et les chaleurs résiduelles sont souvent rejetées dans l'eau ambiante et y affectent sa qualité. Une évaluation précise des processus de mélange turbulent et de dispersion est un des facteurs clés pour l'estimation de l'impact de ces décharges sur l'environnement. Pour ce faire, un modèle numérique tridimensionnel a été développé avec la méthode de simulation des grandes échelles. Dans cette méthode, on calcule explicitement les grands tourbillons et la turbulence de sous-maille est modélisée. L'empirisme lié à la spécification des coefficients de dispersion et de mélange turbulent est donc réduit au minimum. Dans la solution en différences finies, les équations sont décomposées en trois parties : convection, dispersion et propagation. La partie convective est résolue par un schéma basé sur les caractéristiques. La partie diffusive est résolue avec la méthode des différences centrées, et la partie propagation est résolue implicitement en utilisant la méthode itérative de Gauss-Seidel. Le modèle a été appliqué à la simulation d'une ligne source continue dans un écoulement cisailé à surface libre. Les résultats calculés démontrent l'existence de la région de dispersion et de diffusion non Fickiennes au voisinage de la source. Plus loin en aval le processus de diffusion transversale obéit à la loi de Fick, et le coefficient de diffusion transversale est en accord avec la valeur empirique mesurée en laboratoire. La région de diffusion et dispersion initiales non Fickiennes est analysée plus avant sur la base de la cohérence des données de vitesse. On trouve que le coefficient de dispersion suit la loi en puissance $4/3$ d'Okubo, mais avec un coefficient beaucoup plus grand dû à l'effet de cisaillement.

KEYWORDS: Large Eddy Simulation, Scalar transport, Dispersion, Free surface flow.

Introduction

Ambient waters are frequently used to receive municipal and industrial wastewater, as well as to provide cooling water for the dilution of waste heat discharged from power plants and other industries. An accurate evaluation of the turbulent mixing process is one of the key factors for assessing the environmental impact of these discharges. In coastal waters where the flow can be considered unbounded, the rigorous relation between the large scale turbulent eddy viscosity or dispersion and the flow condition is difficult to obtain. Field works were done to determine the dispersion coefficient in ocean and coastal waters (e.g. Okubo, 1975, List et al, 1990). The results displayed a $4/3$ power relationship between the dispersion coefficient and the marked cloud size. However, the measured data are quite scattered and the uncertainty is large. When the cloud size reaches a scale which is several times greater than the length scale of the bounded water body, the dispersion coefficient becomes constant (e.g. Fischer et al., 1979). It is difficult to determine the transition from the initial regime in which the diffusion process obeys the Okubo $4/3$ power law to the final regime in which the diffusion coefficient is con-

stant. To reduce the degree of empiricism in the specification of the dispersion coefficient, the large scale turbulent motion and the associated scalar transport is better to be computed explicitly. This can be achieved by using the technique of Large Eddy Simulation (LES).

LES is by definition three-dimensional. In simulating complex flow phenomena, the specification of boundary and initial conditions needs special attention. The treatment of free surface boundary condition is difficult, and free surface flow problems are relatively seldom tackled by the method of LES. In free-surface shallow water flow, one approach is to use the rigid-lid assumption (Thomas and Williams, 1995). Another approach is to account for the variation of the free water surface by vertically integrating the continuity equation, and relate the variation of the free water surface to the pressure gradient through the hydrostatic pressure assumption (Babajimopoulos and Bedford, 1980).

In the present work, a LES model developed for the simulation of free surface shallow water flow (Li & Wang, 2000) will be extended to include the simulation of scalar transport. An operator splitting method is used so that different numerical schemes can

Revision received March 6, 2001. Open for discussion till October 31, 2002.

be used to approximate different physical processes (e.g. Li & Yu, 1996). The governing equations are split into three parts in the solution: advection, dispersion and propagation. In the advection part the advective accelerations are approximated by the four-node minmax-characteristics scheme (Li, 1990). In the dispersion step the sub-grid scale terms are solved by central difference and the third order Leonard terms are solved by third order difference. In the propagation step the surface elevation (pressure) is obtained from the solution of the Poisson type equation. The model will be tested against the results derived from laboratory and field measurements.

Governing equations

Flow equations

The Navier-Stokes equations for fluid motion are spatially filtered to separate the resolved or large scale field from the subgrid scale field. Denoting the velocity field by a Cartesian vector U_i , the pressure by P , the kinematic viscosity by ν , the space vector by x_i , time by t , and the filtering process by an overbar, the governing equations gives

$$\frac{\partial \bar{U}_i}{\partial x_i} = 0 \quad (1)$$

$$\frac{\partial \bar{U}_i}{\partial t} + \frac{\partial(\bar{U}_i \bar{U}_j)}{\partial x_j} = -\frac{1}{\rho} \frac{\partial \bar{p}}{\partial x_i} + \nu \frac{\partial^2 \bar{U}_i}{\partial x_j \partial x_j} \quad (2)$$

The nonlinear advective term is written as

$$\overline{U_i U_j} = (\bar{U}_i + u_i')(\bar{U}_j + u_j') = \bar{U}_i \bar{U}_j + \overline{u_i' u_j'} + \bar{U}_i u_j' + u_i' \bar{U}_j = \bar{U}_i \bar{U}_j + R_{ij} \quad (3)$$

The first term represents the large scale components and is decomposed by a Taylor series expansion of the filter convolved with the product.

$$\overline{U_i U_j} = \bar{U}_i \bar{U}_j + \frac{\Delta_k}{4\gamma} \frac{\partial^2}{\partial x_k^2} (\bar{U}_i \bar{U}_j) \quad (4)$$

The cross product terms are subsumed into the subgrid scale components and their summation is denoted by R_{ij} .

$$R_{ij} = \tau_{ij} + \frac{1}{3} \delta_{ij} R_{kk} \quad (5)$$

The SGS stress is decomposed into the sum of a trace-free tensor and a diagonal tensor which is absorbed into the pressure term. The trace-free tensor is usually closed by the Smagorinsky eddy viscosity model (Smagorinsky, 1963)

$$\tau_{ij} = -\nu_T \left(\frac{\partial \bar{U}_i}{\partial x_j} + \frac{\partial \bar{U}_j}{\partial x_i} \right) = -2\nu_T S_{ij} \quad (6)$$

$$\nu_T = L^2 \sqrt{2S_{ij} S_{ij}} \quad (7)$$

$$L = C_s [1 - \exp(-x_k^+ / A^+)] (\Delta_1 \Delta_2 \Delta_3)^{1/3} \quad (8)$$

where L is the turbulence characteristic length scale and is modified by the van Driest damping (1956) to account for the effects of solid wall boundaries.

By assuming hydrostatic pressure and neglecting the effects of wind and Coriolis force, the filtered equations of motions are:

$$\frac{\partial \bar{U}_i}{\partial t} + \frac{\partial(\bar{U}_i \bar{U}_j + \frac{\Delta_k}{4\gamma} \frac{\partial^2}{\partial x_k^2} (\bar{U}_i \bar{U}_j))}{\partial x_j} = -\frac{1}{\rho} \frac{\partial \bar{P}}{\partial x_i} + \nu \frac{\partial^2 \bar{U}_i}{\partial x_j \partial x_j} - \frac{\partial(-2\nu_T S_{ij})}{\partial x_j} \quad i = 1, 2 \quad (9)$$

$$\frac{\partial \bar{P}}{\partial x_3} = -\rho g \quad (10)$$

The continuity equation is

$$\frac{\partial \bar{U}_i}{\partial x_i} = 0 \quad (11)$$

The variation of free surface is obtained from the hydrostatic pressure equation and the continuity equation:

$$\frac{\partial \eta}{\partial t} = -\frac{\partial}{\partial x_1} \int_{-h}^{\eta} \bar{U}_1 dx_3 - \frac{\partial}{\partial x_2} \int_{-h}^{\eta} \bar{U}_2 dx_3 \quad (12)$$

where $\eta(x_1, x_2)$ = surface elevation. The surface elevation is related to the pressure at $x_3=0$, $P_0=P(x_1, x_2, 0)$ by

$$\frac{\partial P_0}{\partial x_i} = \rho g \frac{\partial \eta}{\partial x_i} \quad (13)$$

Scalar transport equation

Denoting the scalar concentration by C , the molecular diffusion coefficient by D , the filtered mass conservation of a scalar is given by

$$\frac{\partial \bar{C}}{\partial t} + \frac{\partial(\bar{C} \bar{U}_j)}{\partial x_j} = D \frac{\partial^2 \bar{C}}{\partial x_j \partial x_j} \quad (14)$$

The advective term can be rewritten as

$$\overline{C U_j} = (\bar{C} + c')(\bar{U}_j + u_j') = \bar{C} \bar{U}_j + \overline{c' u_j'} + \bar{C} u_j' + c' \bar{U}_j = \bar{C} \bar{U}_j + Q_j \quad (15)$$

The residual scalar flux Q_j is modelled analogously by

$$Q_j = -\alpha_T \frac{\partial \bar{C}}{\partial x_j} \quad (16)$$

$$\alpha_T = \nu_T / \text{Pr}_i \quad (17)$$

where α_T is the scalar diffusion coefficient and Pr_t is the turbulent Prandtl number. The value of Pr_t is chosen to be 0.5 which is the optimal value found by Eidson (1985). The final form of the equation is given by

$$\frac{\partial \bar{C}}{\partial t} + \frac{\partial}{\partial x_j} \left(\bar{C} \bar{U}_j + \frac{\Delta_k}{4\gamma} \frac{\partial^2}{\partial x_k^2} (\bar{C} \bar{U}_j) \right) = \frac{\partial}{\partial x_j} \left((D + \alpha_T) \frac{\partial \bar{C}}{\partial x_j} \right) \quad (18)$$

Solution method

The split-operator approach is used in the solution of the governing equations. At each time step, the equations are split into three steps: Advection, Diffusion and Propagation terms. The equations for the Advection step are:

$$\frac{\bar{U}_i^{n+1/3} - \bar{U}_i^n}{\Delta t} = -\bar{U}_j \frac{\partial \bar{U}_i}{\partial x_j} \quad i = 1, 2 \quad (19)$$

$$\frac{\bar{C}^{n+1/3} - \bar{C}^n}{\Delta t} = -\bar{U}_j \frac{\partial \bar{C}}{\partial x_j} \quad (20)$$

The minimax-characteristics scheme (Li, 1990) is used to solve the equations of pure advection. This scheme has been found to be more accurate than the Lax-Wendroff scheme in terms of phase accuracy but requires approximately the same computational effort. The use of accurate advection scheme can reduce the numerical error for short waves, as well as that at the region of sharp velocity gradient, such as the separation zone. The equations for the diffusion step are:

$$\frac{\bar{U}_i^{n+2/3} - \bar{U}_i^{n+1/3}}{\Delta t} = \nu \frac{\partial^2 \bar{U}_i}{\partial x_j \partial x_j} - \frac{\partial(-2\nu_r S_{ij})}{\partial x_j} - \frac{\partial(\frac{\Delta_k}{4\gamma} \frac{\partial^2}{\partial x_k^2} (\bar{U}_i \bar{U}_j))}{\partial x_j} \quad i = 1, 2 \quad (21)$$

$$\frac{\bar{C}^{n+2/3} - \bar{C}^{n+1/3}}{\Delta t} = \frac{\partial}{\partial x_j} \left((D + \alpha_T) \frac{\partial \bar{C}}{\partial x_j} \right) - \frac{\partial(\frac{\Delta_k}{4\gamma} \frac{\partial^2}{\partial x_k^2} (\bar{C} \bar{U}_j))}{\partial x_j} \quad (22)$$

In the diffusion step, the simple four-node centred space scheme is used for the second order diffusion terms and a third order difference scheme is used for the Leonard terms (the last terms on the right hand side of the above equation). The equations for the Propagation Step are:

$$\frac{\eta^{n+1} - \eta^{n+2/3}}{\Delta t} = -\frac{\partial}{\partial x_1} \int_{-h}^{\eta} \bar{U}_1 dx_3 - \frac{\partial}{\partial x_2} \int_{-h}^{\eta} \bar{U}_2 dx_3 \quad (23)$$

$$\frac{\partial \bar{U}_i}{\partial t} = -g \frac{\partial \eta}{\partial x_i} \quad i = 1, 2 \quad (24)$$

Equations (23)-(24) are solved implicitly. The three equations are decoupled through two procedures: First, the unknown flow rates at time step $n+1$ are eliminated by differentiating equations (23) with respect to x (x_1) and y (x_2); Second, the resulting Poisson type equation with essential boundary condition is solved by using the Gauss-Seidel iteration method. Finally the vertical velocity U_3 is computed from the continuity equation.

$$U_3 = \int \left(\frac{\partial U_1}{\partial x_1} + \frac{\partial U_2}{\partial x_2} \right) dx_3 \quad (25)$$

Periodic boundary condition (PBC) is predominately used at the inflow boundary for its easiness of implementation (Deardorff, 1970). This type of boundary condition is appropriate for the present case in which the inflow condition and the outflow condition are identical. At outflow boundary the water depth and velocities are determined from a radiation boundary condition. At solid wall boundary, no-slip boundary condition is used and the wall function technique is applied. At the water surface, the surface shear stresses are set to zero. At the bottom, the magnitudes of the bottom shear stresses are specified by the Manning equation.

The initial condition consists of a mean velocity and depth field, as well as a turbulence field. The vertical variation of the filtered longitudinal velocity is specified as a logarithmic profile with a Manning coefficient n . The transverse filtered velocities, are assumed equal to zero and the water depth is computed based on force balance. The turbulence quantities are imposed to the mean velocity field and are generated by a random number generator.

Dispersion simulation

Scalar transport in free surface uniform shear flow is used as the test case for assessing the performance of the model. The reason is that there are ample experiments being carried out and the results are consistent and conclusive. The major source of turbulence in this situation is from the shear stress at the bottom. The dimensions of the computational domain is 6.4m×0.8m×0.4m. The grid system consists of 161 grid points in the streamwise direction, 41 grid points in the transverse direction and 21 grid points in the vertical direction. The mean velocity is 0.5m/s and the Reynolds number based on the depth and the mean velocity is $Re=2 \times 10^5$. A continuous vertical line source is introduced at the middle of the channel. The method of introduction is that at each time step, a fixed amount of scalar quantity is added to the channel.

The large scale temporal variation of the velocity at a typical point is shown in Fig. 1. The turbulence statistics are collected for the last ten turnover periods. Fig. 2 displays the mean vertical velocity profile at the centre of the computational domain. The agreement between the computed results and the measured results (Nezu and Nakagawa, 1993) is satisfactory. Figs. 3a-d show the

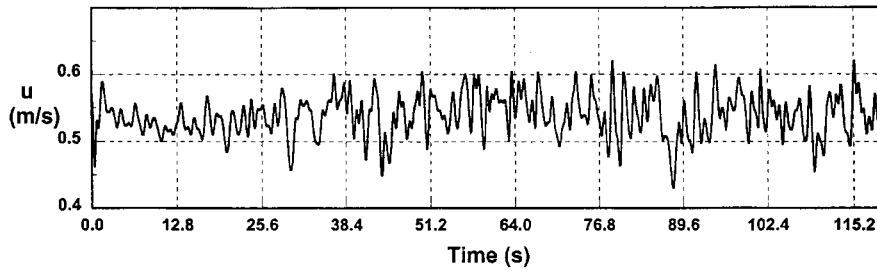


Fig. 1 Temporal variation of velocity variation at a typical point.

distributions of the root mean square (RMS) velocity fluctuations (u', v', w'), and the turbulence kinetic energy (k). The quantities are made non-dimensional by division with the shear velocity u^* or square of u^* , where $u^* = \sqrt{\tau_b/\rho}$ and τ_b is the bottom shear stress. As these quantities are of second order magnitude, the agreement in the results can be considered satisfactory.

The continuous line source is introduced after 100s, when the dynamic steady state of the flow field has been already reached. The time variation of the centreline concentration profile is shown in Fig. 4. The dynamic steady state of the concentration field is achieved after about 110s. The large scale turbulent fluctuation of the scalar concentration is clearly observed. Temporal mean value of the concentration is obtained by averaging the results for a period of 20s after dynamic steady state is attained, and is shown in Fig. 5. Also the analytical solution for two-dimensional turbulent diffusion of a continuous line source in uniform flow is displayed. In the analysis by Elder (1959), a force balance shows that there is a parabolic distribution of the vertical mixing coefficient for momentum. Using the 'Reynolds analogy' the average vertical mixing coefficient is given by

$$\epsilon_z = 0.067u^*H \quad (26)$$

where H =water depth. In the transverse direction, the turbulent diffusion coefficient is expected to have the same order as the vertical diffusion coefficient. However, the width of the channel and thus the transverse velocity profile have a certain effect on

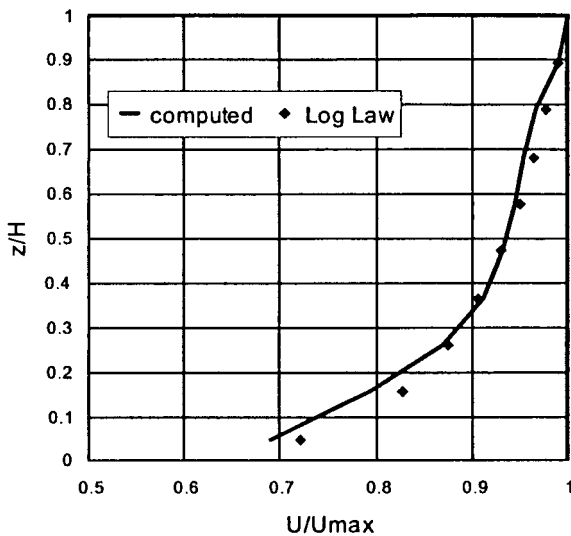
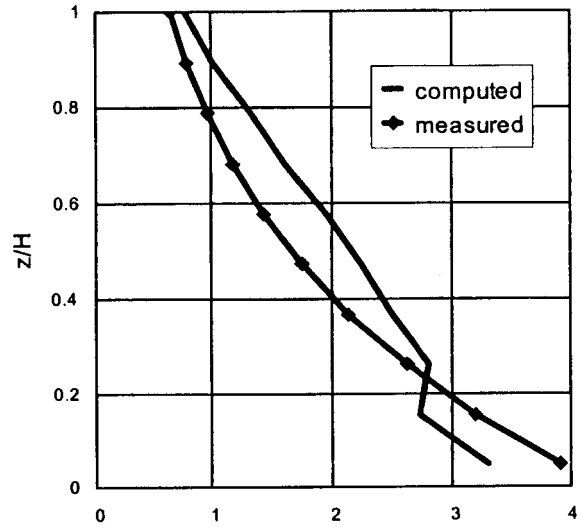
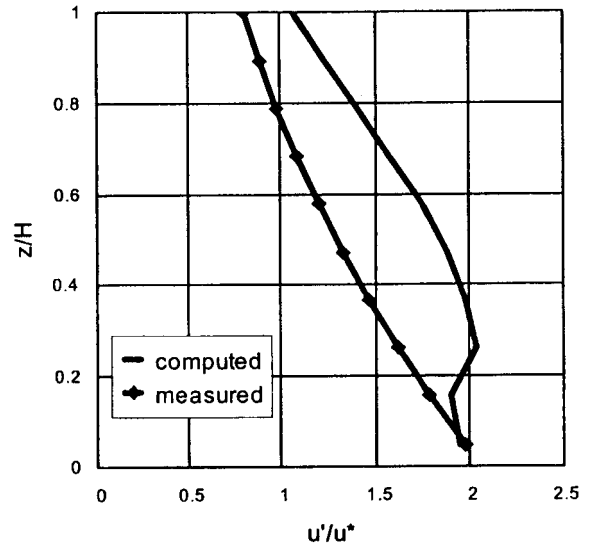


Fig. 2 Mean vertical velocity profile.



3a



3b

the diffusion coefficient. No analytical solution exists and experiments are required. Fischer (1979) reported that there were about 75 experiments done by several investigators (e.g. Elder, 1959, Sullivan, 1968, Okoye, 1970). For smooth channels the experimental results gave

$$\frac{\epsilon_t}{u^*H} = 0.1-0.2 \quad (27)$$

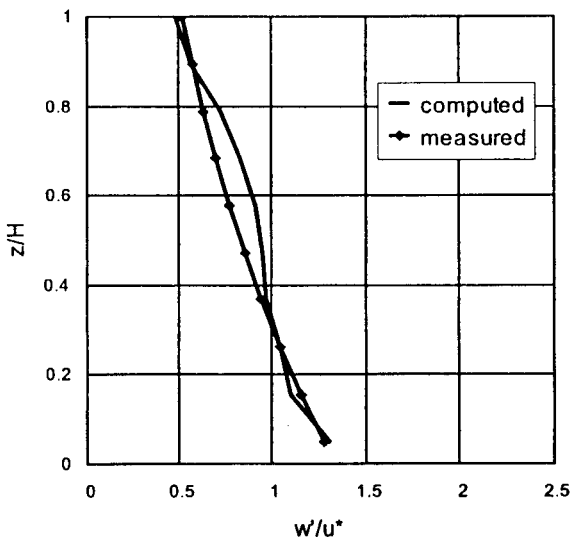
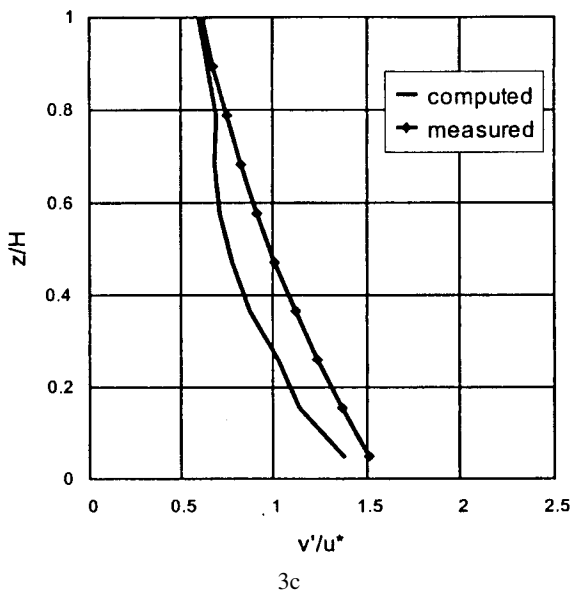


Fig. 3 Vertical profiles of turbulence quantities: a) k , b) u' ; c) v' ; d) w'

In the present LES computations, the transverse turbulence coefficient inferred is $0.1u^*H$, which is the lower bound of the experimental values. It seems that the effect of lateral width on turbulence is not fully accounted for in the present LES model. The disagreement of the two results at the region close to the source indicates that the diffusion is non-Fickian there. It is also partly due to that a distributed source is employed in the computer simulation while a point source is used in the analytical solution. Also the longitudinal dispersion effect is neglected in the analytical solution.

The root mean squares concentration fluctuations roughly equal to 25% of the mean values. The time-averaged computed cross-sectional profile compares favourably with the analytical profile (Fig. 6) and the turbulent scalar flux of the scale concentration in the transverse direction is also in satisfactorily agreement with the analytical solution (Fig. 7). The turbulent scalar flux is obtained by adding the large scale part which is computed explicitly and the subgrid scale part which is modelled by equation (16).

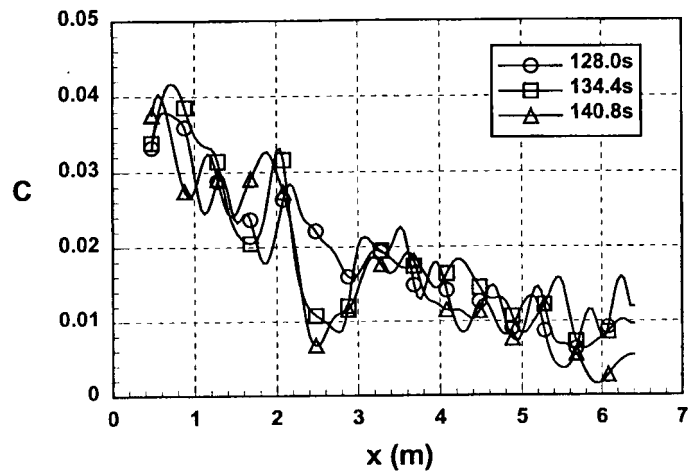


Fig. 4 Temporal variation of centreline concentration.

Non-fickian dispersion

In the above simulation the initial cloud size occupies several grids to avoid numerical difficulties and to reduce numerical error. This means that the initial mixing region in which the diffusion is non-Fickian is too coarse to be reproduced. To resolve the problem, a much finer grid can be used but this is computationally expensive for the present case. An alternative approach is to derive the diffusion coefficient based on the coherence of velocity data. For Lagrangian particle dispersion, Batchelor (1952) showed that

$$K_x = \frac{1}{2} \frac{\partial \sigma_x^2}{\partial t} = \int_0^T \overline{u'(t)u'(t+\tau)} d\tau \quad (28)$$

where σ_x is the variance of a marked cloud of fluid in x -direction, u' is the relative velocity between particles and the average is taken over a sufficiently large number of particles. Winant (1983) demonstrated that this equation is also valid for Eulerian statistics and performed the analysis from paired current meter data. In Eulerian framework, the above equation is modified to

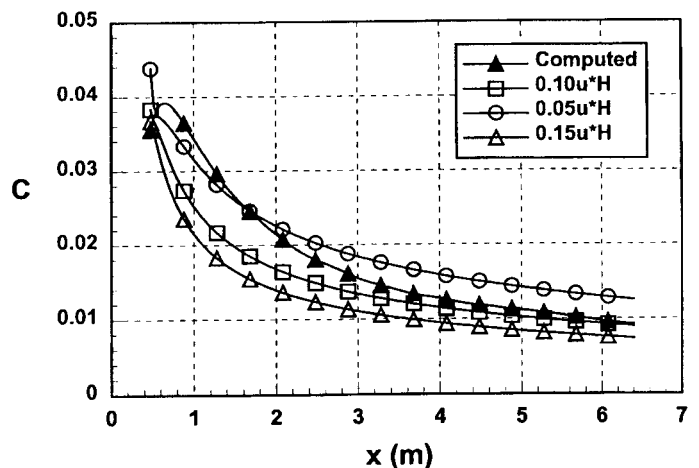


Fig. 5 Time averaged centreline concentration.

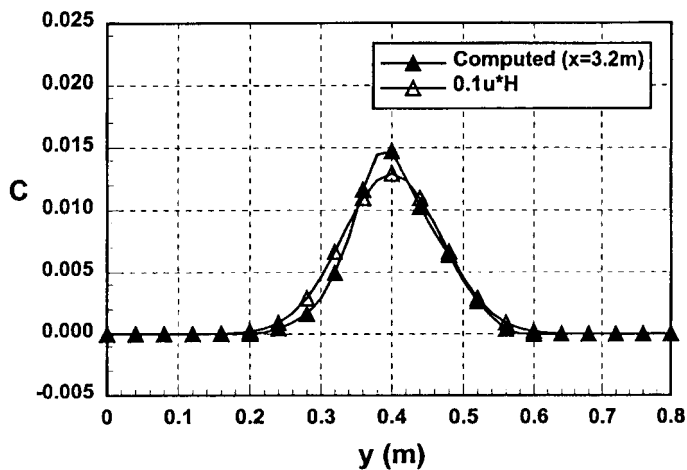


Fig. 6 Temporal mean concentration profile at a cross-section.

$$K_x = \int_0^T \overline{[\delta u(t) - \delta u][\delta u(t + \tau) - \delta u]} d\tau \quad (29)$$

where δu is the difference in velocities at two points. In evaluating the dispersion coefficient, ensemble average is performed by using over 400 data pairs. The typical temporal variation of the ensemble average velocity difference between two points are shown in Figures 8 & 9. The computed dispersion coefficient against the distance of separation between the points (l) are shown in Figure 10.

The best line-of-fit of Okubo's (1975) data is included for comparison. Okubo's data are mainly obtained from the experimental measurement of surface float dispersion in ocean. It is believed that the effect of shear due to bottom friction is not very significant. On the contrary, List et al (1990) carried out float dispersion experiments in coastal areas in which the bottom shear effect is significant. They reported that the field measured dispersion coefficient is two order of magnitude greater than that obtained by Okubo (Figure 11). The bottom shear causes velocity deviation across a cloud, which in turn causes shearing of the cloud, and finally increases the spreading of the cloud. A dimensionally cor-

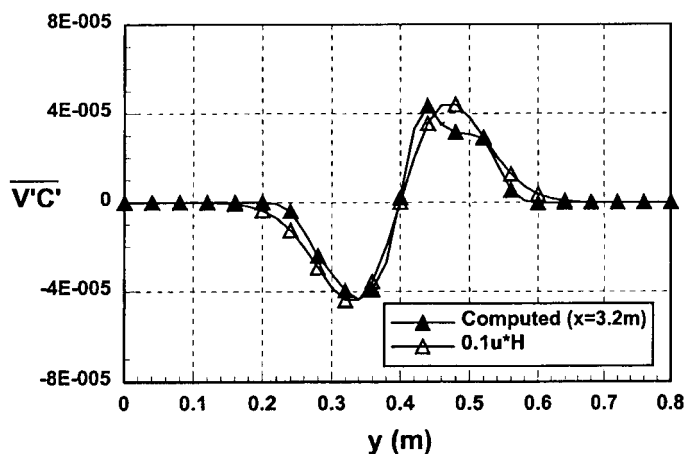


Fig. 7 Temporal mean turbulent scalar flux profile in transverse direction ($\overline{v'c'}$)

rect representation of the dispersion coefficient in this intermediate zone is given by Fischer et al. (1979)

$$K_x \sim \left(\frac{U}{H}\right)^{2/3} \epsilon_z^{1/3} \sigma_x^{4/3} \quad (30)$$

where U/H represents the velocity shear effect, ϵ_z is the turbulent diffusion coefficient in the transverse direction.

The 4/3 power relationship is approximately reproduced by LES in the initial regime which has the scale of the order of the water depth. Also, $U=0.5\text{m/s}$, and $H=0.4\text{m}$, hence $U/H \sim 1$. The above relation thus has been confirmed by the present computations as shown in Figure 10. For List's data, $U \sim 0.2\text{m/s}$, $H \sim 20\text{m}$. Assume $u^* \sim 0.05U$, the above equation also fits quite well the data (Figure 11).

Beyond the initial non-Fickian dispersion regime the dispersion coefficient gradually becomes constant. In the longitudinal direction, the dispersion coefficient is of the same order as that obtained analytically in ideal channel flow ($6u^*H$, Elder, 1959). The dispersion coefficient obtained by Elder (1959) is valid when the cloud already fills the depth and the vertical variation of concentration is small, i.e. well mixed over the depth. The dispersion coefficient can then be represented by a triple integral of the following form.

$$K_x = -\frac{1}{H} \int_0^H u'' \int_0^z \frac{1}{\epsilon_z} \int_0^z u'' dz dz dz \quad (31)$$

In the present work, the dispersion coefficient is obtained from velocity correlation. This approach does not account explicitly for the effect of velocity variation over depth, and is appropriate only for the initial or intermediate zone of the dispersion process. Consequently the computed value is smaller than that obtained from Elder's analysis.

In the transverse direction, the diffusion coefficient is of the same order as that obtained experimentally in ideal channel flow ($0.15u^*H$, Fischer et al., 1979). However, there is some difference in the derived transverse turbulent diffusion coefficients in the Fickian region obtained by continuous source simulation and the coherence analysis of the velocity data. The difference is probably due to the different methods used in deriving the results.

Conclusions

A LES model has been developed and applied to study scalar transport in free-surface shear flow. The model is robust in that the large scale dispersion process is computed explicitly and hence the ad hoc specification of the dispersion coefficient is not required. It can give rich results including time dependent turbulent flow field and concentration field. The simulation results for the case of a continuous line source in shear flow compare favourably with the analytical solution. The derived transverse turbulent diffusivity is close to the average value measured in laboratory. The initial non-Fickian diffusion and dispersion re-

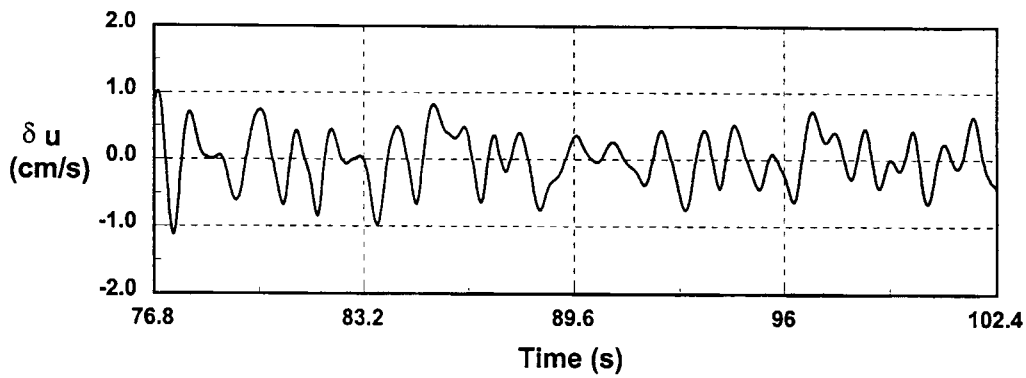


Fig. 8 Temporal variation of the ensemble average velocity difference between two points with separation 4cm in the longitudinal direction (δu).

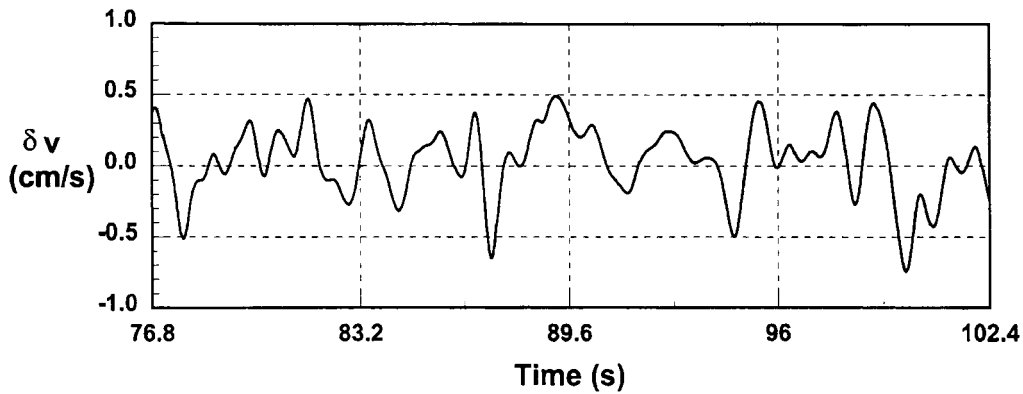


Fig. 9 Temporal variation of the ensemble average velocity difference between two points with separation 4cm in the transverse direction (δv).

gion is reproduced. The derived longitudinal dispersion coefficients based on the coherence of the computed velocity data follow the Okubo's 4/3 power relationship, but with a greater magnitude due to the shear effect.

Acknowledgements

This work was supported by a grant from the Research Grant Council of the Hong Kong Special Administrative Region (Pro-

ject No. 58/96E) and a grant from the Natural Science Foundation of China (Project No. 49676285).

References

- BABAJIMOPOULOS, C., and BEDFORD, K.W., (1980), 'Formulating lake models which preserve spectral statistics', J. Hydraulics Div., ASCE, 106, 1-19.
- BATCHELOR, G.K., (1952), 'Diffusion in a field of homogeneous turbulence. II. The relative motion of particles', Proc. Camb.

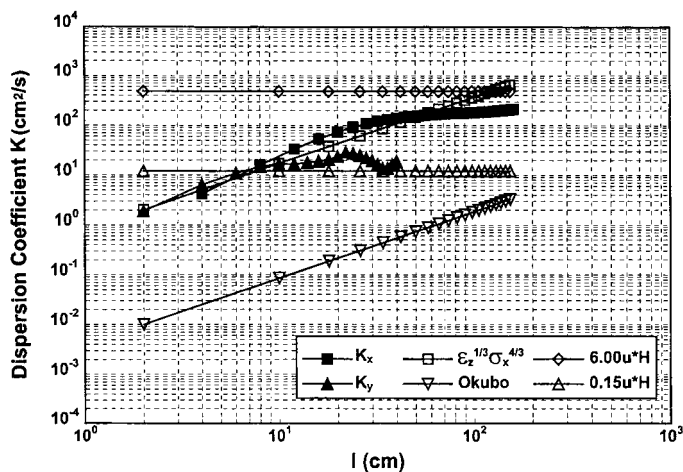


Fig. 10 Variation of dispersion coefficient with length scale (i).

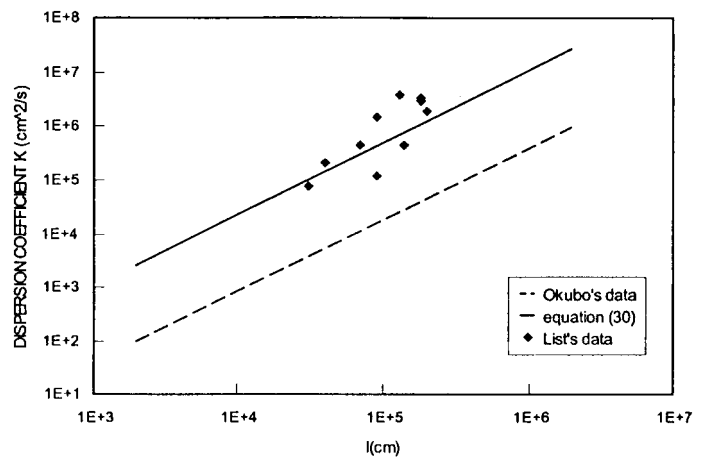


Fig. 11 Variation of dispersion coefficient with length scale (ii).

- Phil. Soc., 48, 345-362.
- DEARDORFF, J.W., (1970), 'A numerical study of three-dimensional turbulent channel flow at large Reynolds numbers', J. Fluid Mech., 41, 453-480.
- EIDSON, T.M., (1985), 'Numerical simulation of turbulent Rayleigh-Benard convection using subgrid scale modelling', J. Fluid Mech., 158, 245-268.
- ELDER, J.W., (1959), 'The dispersion of marked fluid in turbulent shear flow', J. Fluid Mech., 5, 544-560.
- FISCHER, H.B., et al., (1979), *Mixing in Inland and Coastal Waters*, Academic Press, 483 pp.
- LEONARD, B.P., (1979), 'A stable and accurate convective modelling procedure based on quadratic upstream interpolation', Comput. Methods Appl. Mech. Eng., 19, 59-98.
- LI, C.W., (1990), 'Advection simulation by minimax characteristics method', J. Hydraul. Eng. ASCE, 9, 1138-1144.
- LI, C.W. and WANG, J.H., (2000), 'Large eddy simulation of free surface shallow water flow', International Journal for Numerical Methods in Fluids, vol. 34, 1, 31-46.
- LI, C.W. and YU, T.S., (1996), 'Numerical investigation of shallow recirculating flows by a quasi-three-dimensional k- ϵ model', International Journal for Numerical Methods in Fluids, 23, 485-501.
- LIST, E.J., GARTELL, G., WINANT, C.D., (1990), 'Diffusion and dispersion in coastal waters', J. Hydr. Engrg., ASCE, 116, 10, 1158-1179.
- NEZU, I. and NAKAGAWA, H. (1993), *Turbulence in open-channel flows*, A.A. Balkema.
- OKOYE, J.K., (1970), Characteristics of transverse mixing in open channel flows, Rep. KH-R- 23, California Institute of Technology, Pasadena, California.
- OKUBO, A., (1975), 'Ocean diffusion diagrams,' Deep-Sea Research, 18, 789-802.
- SMAGORINSKY, J., (1963), 'General circulation experiments with the primitive equations, Part I: The basic experiment', Mon. Wea. Rev., 91, 99-152.
- SULLIVAN, P.J., (1968), 'Dispersion in a turbulent shear flow', PhD. Thesis, Univ. of Cambridge, Cambridge, England
- THOMAS, T.G., and Williams, J.J.R., (1995), 'Large eddy simulation of turbulent flow in an asymmetric compound open channel', J. Hydraulic Research, 33, 27-42.
- VAN DRIEST, E.R., (1956), 'On turbulent flow near a wall,' J. Aero. Sci., 23, 1007-1011, 1956.
- WINNANT, C.D., (1983), 'Longshore coherence of currents on the Southern California shelf during the summer', J. Physical Oceanography, 13, 1, 54-64.